48th AIAA/ASME/ASCE/AHS/ASC Structures, Structural Dynamics, and Materials Conference
23 - 26 April 2007, Honolulu, Hawaii

AIAA 2007-1966

Multi-Objective Six Sigma Approach Applied to Robust Airfoil Design for Mars Airplane

Koji Shimoyama*

University of Tokyo; currently, Tohoku University, Sendai, 980-8577, Japan

Akira Oyama† and Kozo Fujii‡

Japan Aerospace Exploration Agency, Sagamihara, Kanagawa, 229-8510, Japan

A new optimization approach for robust design, design for multi-objective six sigma (DFMOSS) has been developed and applied to robust aerodynamic airfoil design for Mars exploratory airplane. The present robust aerodynamic airfoil design optimization using DFMOSS successfully showed the trade-off information between maximization and robustness improvement in aerodynamic performance by a single optimization run without careful input parameter tuning. The obtained trade-off information indicated that an airfoil with a smaller maximum camber improves robustness of lift to drag ratio, and that with a larger curvature near the shock wave location improves robustness of pitching moment against the variation of flight Mach number.

I. Introduction

In real-world engineering designs, performance of a design may be very different from its expected value due to errors and uncertainties in design process, manufacturing process, and/or operating condition. A typical example of such critical situations is airplane wing design. It is well known that aerodynamic performance of an airplane is very sensitive to the wing shape and flight condition, and inevitable uncertainties such as wing manufacturing errors and wind variations may lead to drastic deterioration in aerodynamic performance of an airplane. In the airplane wing design, therefore, it is required not to use the conventional design optimization approach considering only optimality of performance at the design point, but to use the robust design optimization approach considering both optimality and robustness of performance against any uncertainties. Especially, in the wing design for future Mars airplane[1–3] which has recently attracted attention as a new approach to explore Mars in spite of conventional orbiting satellites and rovers, the use of robust design optimization approach is much more required because the Martian atmosphere has very large wind variations.[4,5]

Indeed, improvements in optimality and robustness are usually competing in real-world design problems. Therefore, not a single, but multiple robust optimal solutions actually exist, such that finding these compromised solutions and revealing the trade-off information between optimality and robustness are both objectives for robust design optimization. The new acquired knowledge can aid the upper-level decision maker to pick one solution from the compromised solutions, together with an additional design consideration.

Up to the present, some robust optimization approaches have been developed and applied to engineering design problems in order to reveal realistic and practical design information.[6–8] Among these, the design for six sigma (DFSS)[6] is one of the most popular robust optimization approaches, due to its simple and practical formulation. DFSS has been successfully applied to various robust optimization problems in various engineering fields.[9,10] However, the DFSS needs careful setting of input parameters, and has difficulty in revealing trade-off information between optimality and robustness of design because it is based on a single-objective optimization method, as is the approach proposed by Deb and Gupta.[7] Another alternative for

*Research Fellow, Institute of Fluid Science, 2-1-1 Katahira, Aoba-ku; shimoyama@edge.ifs.tohoku.ac.jp. Member AIAA.

†Research Associate, Institute of Space and Astronautical Science, 3-1-1 Yoshinodai; oyama@flab.eng.isas.jaxa.jp. Member AIAA.

‡Professor, Institute of Space and Astronautical Science, 3-1-1 Yoshinodai; fujii@flab.eng.isas.jaxa.jp. Fellow AIAA.

robust optimization is the performance measure approach (PMA),[8] proposed by Youn and Choi. Although effective in terms of accuracy and stability, this method probably needs a more intuitive formulation before it becomes popular in the engineering design field for real-world applications.

Objectives of this paper are to propose a new robust design optimization approach "design for multi-objective six sigma (DFMOSS)" by combining the ideas of DFSS and multi-objective evolutionary algorithm (MOEA),[11] and to carry out the robust aerodynamic airfoil design optimizations for future Mars airplane by using the DFMOSS coupled with computational fluid dynamics (CFD) simulation. In this paper, two robust aerodynamic airfoil design optimizations are carried out; the optimization considering robustness of lift to drag ratio against the variation of flight Mach number, and that considering robustness of pitching moment constraint against the variation of flight Mach number. In each robust optimization, the DFMOSS is investigated in terms of efficiency and capability of revealing trade-off information between optimality and robustness of performance, and practical airfoil design information about the improvement in both optimality and robustness of aerodynamic performance against the variation of flight Mach number is suggested for future Mars airplane.

II. Design for Six Sigma

Design for six sigma (DFSS)[6] is based on the "six sigma" concept, which was originally established as a measure of excellence for business processes. The aim is to achieve a process with such a small dispersion that the range of $\pm 6\sigma$ (σ: standard deviation) around the mean value μ is included in an acceptable range for the performance parameter. The level of dispersion can be defined as "sigma level n", as shown in Fig. 1 where larger sigma level indicates smaller dispersion. In the context of robust design optimization, smaller dispersion translates to a more robust characteristic.

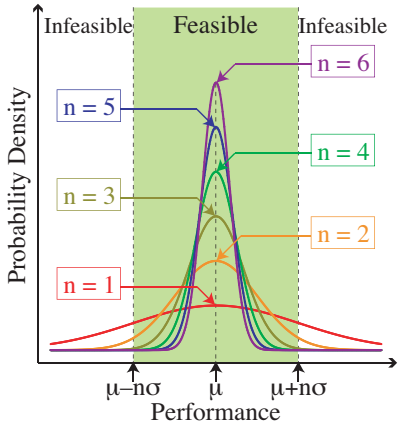

Sigma level n	Safety probability [%]
1	68.25
2	95.46
3	99.73
4	99.9937
5	99.999943
6	99.9999998

Figure 1. Characteristics of sigma level n.

Consider a single-objective non-constrained optimization problem where the value of objective function $f(\boldsymbol{x})$ of design variable $\boldsymbol{x}$ must be minimized as follows:

$$\text{Minimize: } f(\boldsymbol{x}) \tag{1}$$

In robust design optimization using DFSS, Eq. 1 is rewritten to the problem where the weighted summation of the mean value μ_f and the variance ${\sigma_f}^2$ of the objective function must be minimized as follows:

$$\text{Minimize: } w_\mu \mu_f + w_\sigma {\sigma_f}^2 \tag{2}$$

where w_μ and w_σ are user-specified weighting factors of μ_f and ${\sigma_f}^2$, respectively. μ_f and σ_f are estimated by sampling $\boldsymbol{x}$ following its probability distribution and evaluating $f(\boldsymbol{x})$ at each sample point. In DFSS, the following inequality constraints are specified in advance to achieve the expected sigma level quality of the obtained solution, as shown in Fig. 1.

$$\begin{aligned} \text{Subject to: } & \mu_f - n\sigma_f \geq \text{LSL} \\ & \mu_f + n\sigma_f \leq \text{USL} \end{aligned} \tag{3}$$

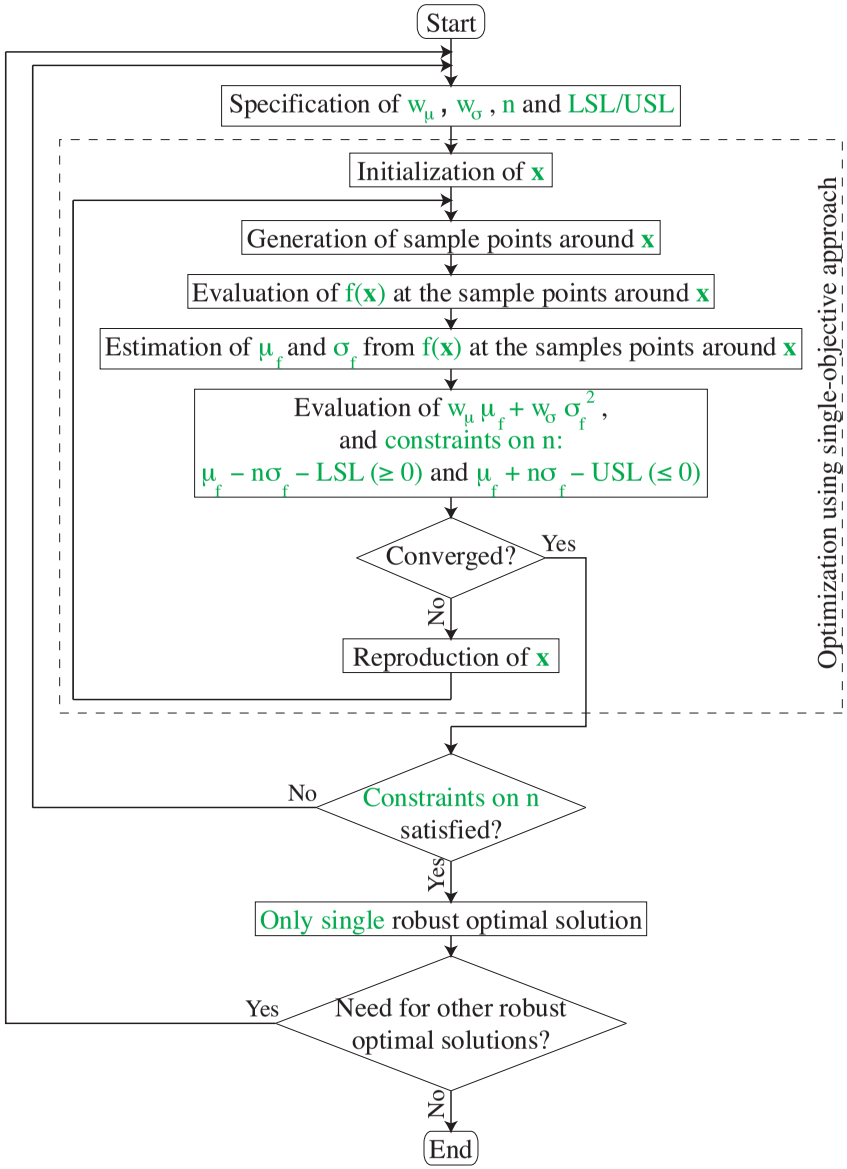

Figure 2. Flowchart of robust optimization using DFSS.

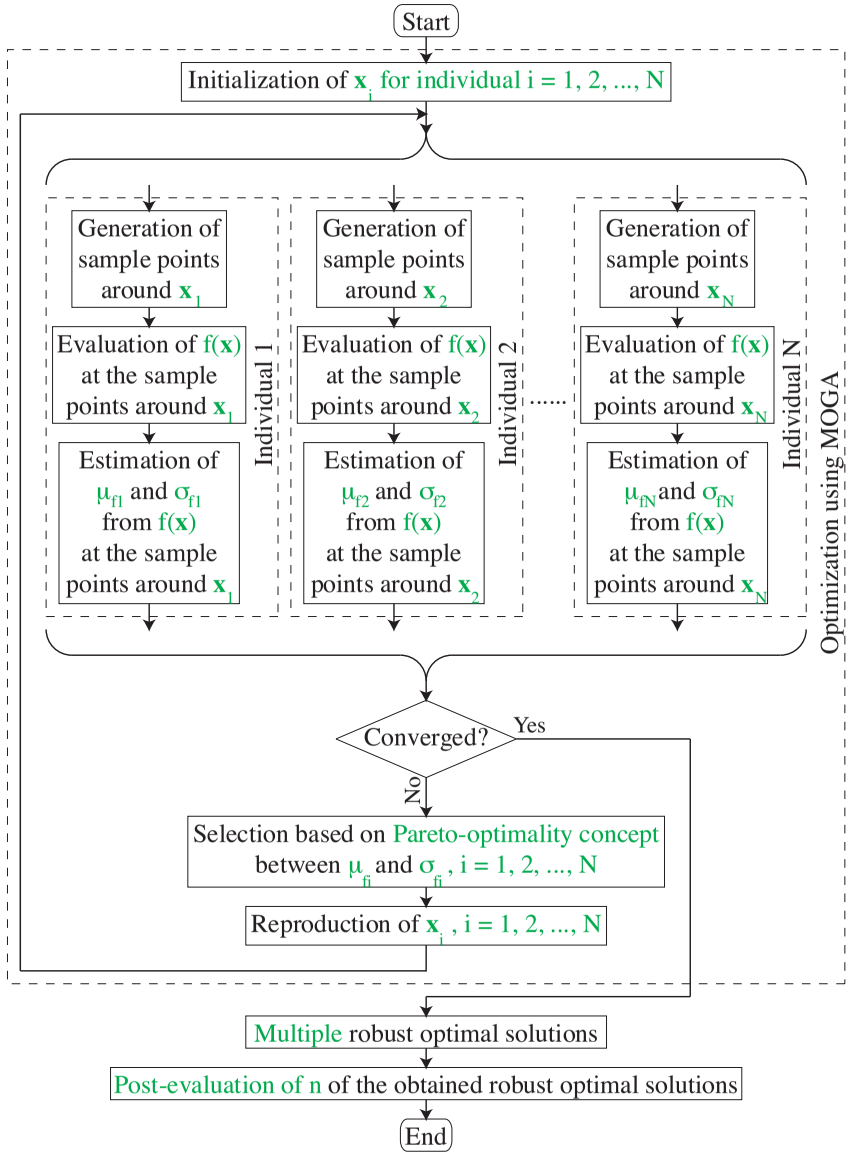

Figure 3. Flowchart of robust optimization using DFMOSS.

where n represents user-specified sigma level, and LSL and USL are user-specified lower and upper objective function limits, respectively.

Figure 2 illustrates the flowchart of robust optimization using DFSS. First, parameters such as weighting factors w_μ and w_σ, sigma level n, and LSL/USL are pre-specified by the user, and then it proceeds to the optimization block. In this block, μ_f and σ_f of $f(\boldsymbol{x})$ at sample points around $\boldsymbol{x}$ are evaluated, and $w_\mu\mu_f + w_\sigma{\sigma_f}^2$ is dealt with as one objective function. Then, $\mu_f - n\sigma_f - \mathrm{LSL}(\geq 0)$ and/or $\mu_f + n\sigma_f - \mathrm{USL}(\leq 0)$ are evaluated as two constraint functions. $\boldsymbol{x}$ for the next step is reproduced based on the evaluated objective and constraint functions, and this optimization process is iterated until $\boldsymbol{x}$ has converged. This single-objective optimization can be carried out by using any single-objective optimization approach.

The DFSS has some limitations as follows. First, it is necessary to pre-specify the weighting factors w_μ and w_σ carefully, even though it is difficult for the user to pre-specify values for weighting factors appropriately because the trade-off information is still unknown. Also, it is necessary to pre-specify an appropriate sigma level n, although essentially, the sigma level satisfying Eq. 3 is known only after an optimization run. Therefore, users must pre-specify the sigma level without any information, while a robust optimal solution may not even be obtainable at the pre-specified value of sigma level. Second, only one robust optimal solution can be obtained in a single optimization run, for the DFSS operates according to the single-objective function given by Eq. 2. As a result, many optimization runs with different values of weighting factors and sigma level must be performed by the user in order to obtain multiple robust optimal solutions, which shall then reveal the trade-off relation between optimality and robustness of performance. Furthermore, the trade-off relation between optimality and robustness may not be derived even after many optimization runs (*e.g.* if the obtained multiple optimal solutions distribute only locally).

III. Design for Multi-Objective Six Sigma

The idea of design for multi-objective six sigma (DFMOSS)[12] is to incorporate multi-objective evolutionary algorithm (MOEA)[11] into DFSS in order to overcome those limitations mentioned above. In DFMOSS, the mean value (μ_f) and the standard deviation (σ_f) of the objective function $f(\boldsymbol{x})$ are dealt with as multiple objective functions and thus minimized separately (for $f(\boldsymbol{x})$ minimization problem) as follows:

$$\begin{matrix} \text{Minimize: } \mu_f \\ \sigma_f \end{matrix} \tag{4}$$

Figure 3 illustrates the flowchart of robust optimization using DFMOSS. There is no need to pre-specify weighting factors w_μ and w_σ before optimization as in DFSS (Fig. 2), because DFMOSS deals with the multi-objective optimization problem given by Eq. 4. There is no need to pre-specify sigma level n either, because DFMOSS does not consider the constraint on sigma level n given by Eq. 3 during the optimization process. The sigma level n satisfying Eq. 3 can be evaluated from the robust optimal solutions in the post-processing, as shown in Fig. 4 (this will be described in the next paragraph). During the optimization process itself, multiple solutions (individuals) $\boldsymbol{x}_1, \boldsymbol{x}_2, \cdots, \boldsymbol{x}_N$ are dealt with simultaneously using MOEA. For each individual $i = 1, 2, \cdots, N$, μ_{f_i} and σ_{f_i} are evaluated as two separate objective functions from $f(\boldsymbol{x})$ at the sample points around $\boldsymbol{x}_i$. Better solutions are selected based on the Pareto-optimality concept between μ_{f_i} and σ_{f_i} for $i = 1, 2, \cdots, N$. Solutions $\boldsymbol{x}_1, \boldsymbol{x}_2, \cdots, \boldsymbol{x}_N$ for the next step are reproduced by crossover and mutation from the selected solutions. This optimization process is iterated until the trade-off relation between μ_f and σ_f has converged, and multiple robust optimal solutions are obtained.

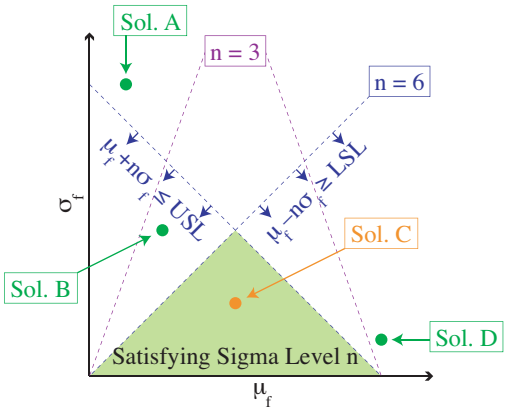

Figure 4. Post-evaluation of sigma level n.

The post-evaluation of sigma level n is illustrated in Fig. 4, where four robust optimal solutions (A, B, C and D) obtained by a DFMOSS optimization were taken as example. The shaded region indicates the area satisfying the constraint of 6σ robustness quality, i.e. points included in this region (solution C) have robustness quality equal to or above 6σ. Points outside this region (solutions A, B and D) do not satisfy the constraint of 6σ robustness quality. Solution B for instance, is included in the area satisfying the constraint

of 3σ robustness quality, thus inferior to solution C in terms of robustness. Therefore, the satisfied sigma level of each obtained robust optimal solution can be evaluated in a flexible sense, considering the trade-off between optimality and robustness of design.

IV. Robust Aerodynamic Airfoil Design for Future Mars Airplane

IV.A. Problem Definition

In this study, robust aerodynamic airfoil design optimizations against the variation of flight Mach number for a future Mars airplane are carried out to investigate the efficiency and capability of DFMOSS to reveal trade-off information between optimality and robustness of aerodynamic performance. The cruising flight condition of NASA's "Airplane for Mars Exploration (AME)",[1] shown in Fig. 5, is adopted as the present design point; Reynolds number based on root chord length $Re = 1.0 \times 10^5$, freestream Mach number $M_\infty = 0.4735$, and the angle of attack $\alpha = 2.0$ [deg]. In addition, it is assumed that M_∞ disperses around the design point of 0.4735 in a normal distribution with a standard deviation of 0.1. Here, the value of 0.1 as the standard deviation of M_∞ is nearly equal to the daily and seasonal variations of about 22 m/s in the speeds of westerly winds at the altitude of several kilometers over Mars,[4] where the airplane is assumed to fly. In this study, two robust aerodynamic airfoil design optimizations for future Mars airplane are carried out; Case 1: considering robustness of lift to drag ratio L/D (L is lift and D is drag), and Case 2: considering robustness of pitching moment coefficient constraint $|C_{Mp}| \leq 0.13$ ($C_{Mp} = M_p/(\frac{1}{2}\rho_\infty {u_\infty}^2 S_{ref} c_{ref})$ is pitching moment coefficient, M_p is pitching moment around 25 % chord position, ρ_∞ is freestream density, u_∞ is freestream velocity, S_{ref} is the wing area and c_{ref} is the root chord length). Case 1 aims at finding the airfoil configuration which can assure the expected flight range, and Case 2 aims at finding one which can assure controllability of pitching motion by its horizontal tail wing when the flight Mach number disperses widely around its design point.

Figure 5. NASA's "Airplane for Mars Exploration (AME)."[1]

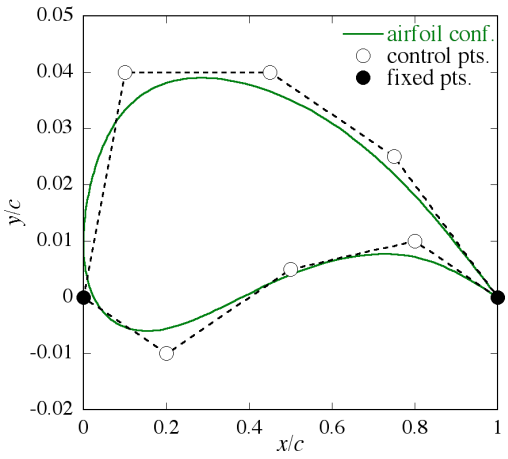

Figure 6. Definition of airfoil configuration based on the B-spline curves.

In both cases, airfoil configuration is defined by the B-spline curves with three fixed points corresponding to the leading and trailing edges and six control points whose coordinates can be specified flexibly, as shown in Fig. 6 (here, c is the airfoil chord length). The design variables are chordwise (x) and vertical (y) coordinates of the six control points, therefore the number of design variables is twelve. Such definition based on the B-spline curves has some advantages; the second-order derivative of coordinate along the B-spline curves is continuous, various airfoil configurations can be expressed, and definition of initial design space is intuitive.[13] The structural constraint on airfoil thickness is not considered because we want to discuss an aerodynamic effect purely in the present study.

IV.B. Case 1: Considering Robustness of Lift to Drag Ratio

The present robust optimization problems using DFSS and DFMOSS are defined, respectively, as follows:

- Robust optimization using DFSS

  When M_∞ disperses around 0.4735 following the normal distribution with its standard deviation of 0.1,

  - Minimize: $-\ w_\mu \cdot$ (mean value of L/D) $+ w_\sigma \cdot$ (variance of L/D)

– Subject to: (mean value of L/D) $- n \cdot$ (standard deviation of L/D) ≥ 42

- Robust optimization using DFMOSS

  When M_∞ disperses around 0.4735 following the normal distribution with its standard deviation of 0.1,

  – Maximize: mean value of L/D

  – Minimize: standard deviation of L/D

These robust optimization problems are solved by using the DFSS based on a single-objective EA (SOEA), and the DFMOSS based on a MOEA, respectively. Fitness values are evaluated by using a Pareto-ranking method,[14] a fitness sharing,[11,14] and the Michaleswicz's nonlinear function[15] in DFMOSS while a standard ranking method and the Michaleswicz's nonlinear function are used in DFSS. Parents are selected by the stochastic universal sampling (SUS).[16] Children are reproduced by the blended crossover (BLX-0.5) method[17] and uniform mutation[11] set at a rate of 20 % and maximum perturbation range of 10 % of the design space. The alternation of generations is performed by the best-N selection.[18,19] Population size and number of generations are 64 and 100, respectively. The statistical values of objective function such as μ_f and σ_f against dispersive design variables $\boldsymbol{x} = [x_1, x_2, \cdots, x_M]^T$ are estimated by the second-order Taylor's series expansion approach given as

$$\begin{aligned} \mu_f &= f(\boldsymbol{\mu_x}) + \frac{1}{2}\sum_{i=1}^{M} \frac{\partial^2 f}{\partial {x_i}^2} \sigma_{x_i} \\ \sigma_f &= \sqrt{\sum_{i=1}^{M} \left(\frac{\partial f}{\partial x_i}\right)^2 {\sigma_{x_i}}^2 + \frac{1}{2}\sum_{i,j=1}^{M} \left(\frac{\partial^2 f}{\partial x_i \partial x_j}\right)^2 {\sigma_{x_i}}^2 {\sigma_{x_j}}^2} \end{aligned} \tag{5}$$

where $\boldsymbol{\mu_x}$ is a vector of user-specified mean values of $\boldsymbol{x}$, and σ_{x_i} is user-specified standard deviation of the i-th dispersive design variable. The first and the second derivatives of $f(\boldsymbol{x})$ with respect to x_i in Eq. 5 are evaluated by central differencing. The present dispersive design variable corresponds to the flight Mach number M_∞, therefore, $M = 1$, $x = M_\infty$, $\mu_x = 0.4735$ and $\sigma_x = 0.1$, and μ_f and σ_f are estimated from $f(x)$ evaluated at three conditions $x = M_\infty = 0.3735$, 0.4735 and 0.5735.

In the robust optimization using DFSS, the sigma level n is set to 3σ, and the constraint on sigma level n is dealt with by using the Pareto-optimality-based constraint-handling (PBCH) technique.[20] Three optimization runs using DFSS with different weighting factors ($w_\mu : w_\sigma = 1:10$, $1:1$ and $10:1$) are performed. In the robust optimization using DFMOSS, on the other hand, only one optimization run is performed without any pre-specification of weighting factors and sigma level. Here note that computation time taken by one optimization run using DFSS is nearly equal to that using DFMOSS. This means that three present robust optimization runs using DFSS take about three times as much total computation time as one present robust optimization run using DFMOSS.

Aerodynamic performance of an airfoil is evaluated by computational fluid dynamics (CFD) simulation. The governing equations for CFD simulation are two-dimensional Farve-averaged compressible thin-layer Navier-Stokes equations. The LU-ADI factorization algorithm[21] is used for the time integration. The inviscid terms of numerical fluxes are evaluated by the SHUS scheme.[22] In the inviscid terms, high-order accuracy is obtained by the third-order upwind-biased MUSCL interpolation[23] based on the primitive variables with van Albada differentiable limiter.[24] The viscous terms are evaluated by the second-order central differencing, and the turbulent viscosity is modeled by the Baldwin-Lomax algebraic turbulence model.[25] In the present study, C type grid as shown in Fig. 7 is used. The number of grid points is 251 in the direction around the airfoil (211 points over the airfoil surface), 51 in the direction normal to the airfoil surface, and the total number of grid points is 12,801.

The computational time required for one evaluation of aerodynamic performance of an airfoil using the CFD simulation is about five minutes with one processor of NEC SX-6 computing system owned by the Institute of Space and Astronautical Science (ISAS) of Japan Aerospace Exploration Agency (JAXA). In the present study, the optimizer distributes the multiple evaluators corresponding to the multiple individuals of EA into 32 processors of this computing system in parallel. Therefore, the total computation time required for one present robust aerodynamic design optimization run using DFMOSS can be reduced to about 56 hours, while it takes about 135 hours to perform the present three robust optimization runs using DFSS.

Figure 8 compares the robust optimal solution distributions (standard deviation of L/D against mean value of L/D) obtained through DFSS and DFMOSS. The DFSS found three robust optimal solutions with more than 3σ robustness quality. However, these solutions distribute narrowly and sparsely. This indicates that the DFSS has lack in capability of revealing global trade-off relation between optimality (mean value of L/D) and robustness (standard deviation of L/D), and the DFSS requires more optimization runs with different combinations of weighting factors to obtain more detailed trade-off information. Fortunately, in the present optimizations using DFSS, three robust optimal solutions can be obtained because the pre-specified value of sigma level as 3σ is appropriate by chance. However, it is not always guaranteed for the DFSS to obtain the robust optimal solutions according to pre-specification of sigma level. On the other hand, the DFMOSS found multiple (total eighteen) robust optimal solutions distributing globally and uniformly in the design space by a single optimization run. From this robust optimal solution distribution obtained through DFMOSS, global trade-off information between optimality and robustness can be understood easily; *e.g.*, the maximum sigma level of L/D of the obtained solutions is more than 6σ by the post-evaluation when the lower specification limit of L/D is set to 42, and the standard deviation of L/D increases drastically when the mean value of L/D becomes larger than 44.5. In the present case, the robust optimization using DFSS found better robust optimal solutions (located in lower right in Fig. 8) than that using DFMOSS. This is because the DFMOSS searched an unexpectedly larger design space, i.e., producing unpractical solutions with good robustness but extremely bad optimality of L/D. However, such situation can be avoided easily by adding some constraints which eliminate unpractical design space.

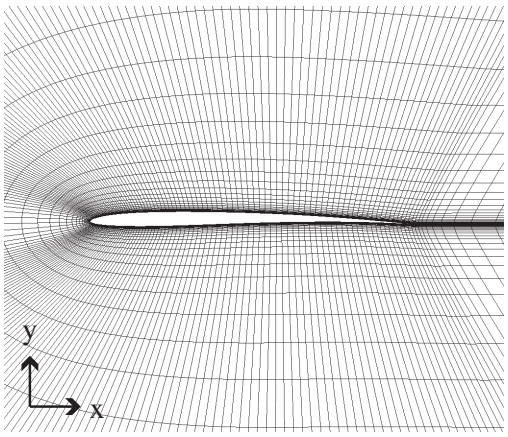

Figure 7. Grid distribution.

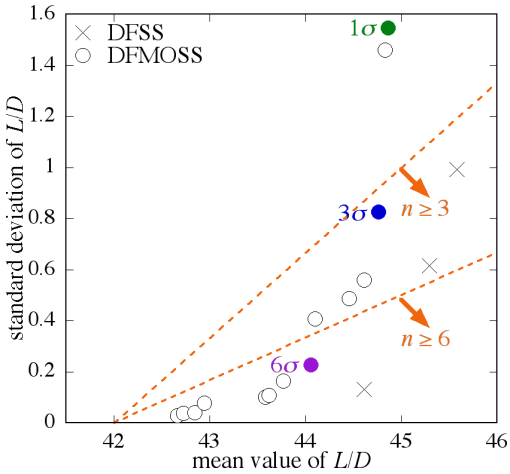

Figure 8. Comparison of robust optimal solutions obtained through DFSS and DFMOSS in Case 1.

Hereafter, three robust optimal solutions with 1σ, 3σ and 6σ robustness qualities of L/D obtained through DFMOSS (shown by closed circles in Fig. 8) are compared and discussed. First, Fig. 9(a) shows the histories of L/D against M_∞ at $\alpha = 2.0$ [deg] of these three robust optimal solutions. In the robust optimal solution with 1σ robustness quality, L/D decreases drastically with an increment in M_∞, and it falls below its lower specification limit of 42 at high M_∞. On the other hand, the robust optimal solution with larger sigma level has slightly smaller L/D at the design point $M_\infty = 0.4735$, but more stable characteristics keeping large L/D against the increment in M_∞. These results prove that the present robust aerodynamic design optimization using the DFMOSS could actually find the multiple airfoil designs with various robustness qualities of L/D against the variation of M_∞ by a single optimization run.

Next, Fig. 9(b) shows the airfoil configurations of these three robust optimal solutions with 1σ, 3σ and 6σ robustness qualities obtained through DFMOSS. It indicates that maximum camber is one of the major trade-off factors between L/D and robustness improvements. The reason is that an airfoil with a smaller maximum camber realizes a smaller increment in pressure drag due to shock wave, and eventually improves the robustness in L/D against the increment in M_∞.

IV.C. Case 2: Considering Robustness of Pitching Moment Constraint

The present robust optimization problems using DFSS and DFMOSS are defined, respectively, as follows:

- Robust optimization using DFSS

  When M_∞ disperses around 0.4735 following the normal distribution with its standard deviation of 0.1,

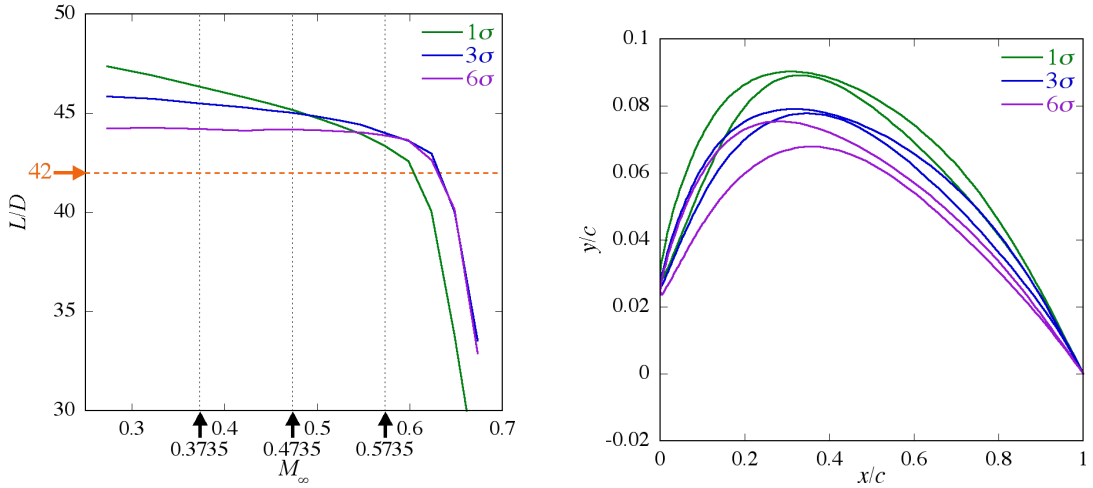

(a) L/D histories against M_∞.

(b) Airfoil configurations.

Figure 9. Three robust optimal solutions obtained through DFMOSS in Case 1.

  - Maximize: mean value of L/D
  - Subject to: $|\text{mean value of } C_{Mp}| + n \cdot (\text{standard deviation of } C_{Mp}) \leq 0.13$

- Robust optimization using DFMOSS

  When M_∞ disperses around 0.4735 following the normal distribution with its standard deviation of 0.1,

  - Maximize: mean value of L/D
  - Maximize: $n = -\frac{|\text{mean value of } C_{Mp}| - 0.13}{\text{standard deviation of } C_{Mp}}$

In both robust optimizations, the following constraint is considered at the design point $M_\infty = 0.4735$:

- Subject to: $|C_{Mp}| \leq 0.13$

Case 2 corresponds to the optimization that considers the robustness in constraint function ($|C_{Mp}| \leq 0.13$) violation, while the optimization in Case 1 considers the robustness in objective function (L/D). Therefore, the formulation of robust optimization problem in Case 2 is also slightly different from that in Case 1. However, Case 2 is similar to Case 1 as DFSS needs the pre-specification of sigma level n and deals with the single-objective optimization problem, while DFMOSS deals with the multi-objective optimization problem with separate objective functions corresponding to optimality (mean value of L/D) and robustness (sigma level of $|C_{Mp}| \leq 0.13$).

The optimizer and the CFD solver used in Case 2 are the same as those used in Case 1. In the robust optimization using DFSS, three optimization runs with different sigma level ($n = 1\sigma$, 3σ and 6σ) are carried out. In the robust optimization using DFMOSS, only one optimization run is performed without pre-specification of sigma level n (n can be derived from the mean value and the standard deviation of C_{Mp} which are evaluated during optimization process).

Figure 10 compares the robust optimal solution distributions (sigma level of $|C_{Mp}| \leq 0.13$ against mean value of L/D) obtained through DFSS and DFMOSS. The DFSS found three robust optimal solutions corresponding to pre-specified sigma levels (1σ, 3σ and 6σ), respectively. However, these solutions distribute sparsely. Therefore, it can be said that the DFSS requires more optimization runs with different sigma levels to obtain more detailed trade-off information between optimality (mean value of L/D) and robustness (sigma level of $|C_{Mp}| \leq 0.13$), which is similar to the result in Case 1. On the other hand, the DFMOSS found multiple (total forty) robust optimal solutions distributing globally and uniformly in the design space by a single optimization run. In addition, the DFMOSS found the greatly robust optimal solutions which exceeded far more than the maximum pre-specified sigma level as 6σ successfully. These indicate that the DFMOSS has an excellent capability of finding robust optimal solutions.

Hereafter, three robust optimal solutions with 1σ, 4σ and 8σ robustness qualities of $|C_{Mp}| \leq 0.13$ obtained through DFMOSS (shown by closed circles in Fig. 10) are compared and discussed. First, Fig. 11(a) shows the histories of C_{Mp} against M_∞ at $\alpha = 2.0$ [deg] of these three robust optimal solutions. In the robust optimal solution with 1σ robustness quality, C_{Mp} is larger than its lower limit of -0.13 at the design point $M_\infty = 0.4735$, but C_{Mp} falls below -0.13 and the constraint $|C_{Mp}| \leq 0.13$ is not satisfied at high M_∞. On the other hand, the robust optimal solutions with larger sigma level has slightly more stable characteristics of C_{Mp} against an increment in M_∞ and its history of C_{Mp} against M_∞ shift upper from -0.13 to satisfy the constraint $|C_{Mp}| \leq 0.13$ even at high M_∞. These results indicate that the robust aerodynamic design optimization using the DFMOSS could actually find the multiple designs with various robustness qualities of C_{Mp} against the variation of M_∞ by a single optimization run.

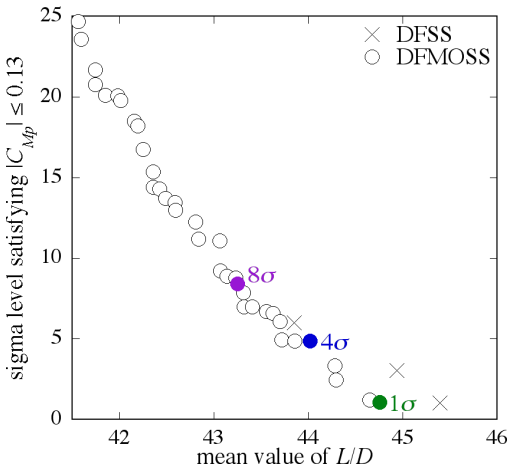

Figure 10. Comparison of robust optimal solutions obtained through DFSS and DFMOSS in Case 2.

Next, Fig. 11(b) shows the airfoil configurations of these three robust optimal solutions with 1σ, 4σ and 8σ robustness qualities obtained through DFMOSS. It is seen that the airfoil is folded down more greatly at about 15 % chord position, corresponding to the location of shock wave occurring at higher M_∞, as the sigma level becomes larger. Such an airfoil suppresses the backward movement of shock wave, and eventually realizes smaller variation, i.e., more robust characteristic of C_{Mp} against the increment in M_∞.

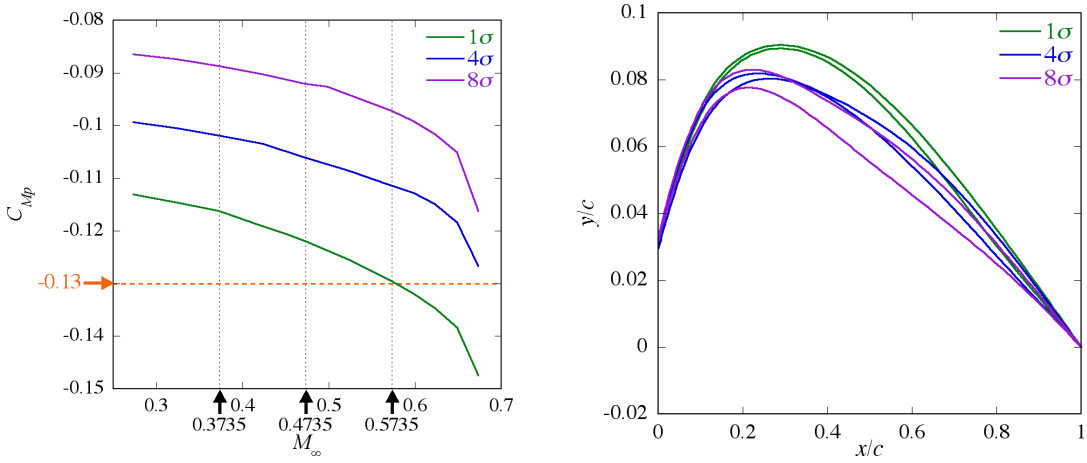

(a) C_{Mp} histories against M_∞. (b) Airfoil configurations.

Figure 11. Three robust optimal solutions obtained through DFMOSS in Case 2.

V. Concluding Remarks

In this paper, a new robust optimization approach called DFMOSS has been proposed by incorporating the idea of MOEA into DFSS, and the robust aerodynamic airfoil design optimizations for future Mars airplane have been carried out by using the DFMOSS coupled with the CFD simulation. Compared to DFSS, the present robust optimizations using DFMOSS effectively revealed more detailed trade-off information between the optimality and the robustness of aerodynamic performances by a single optimization run without careful tuning of input parameters such as weighting factors and sigma level. Then, the obtained trade-off information was discussed, and practical airfoil design concepts considering the robustness of aerodynamic performances have been obtained; an airfoil with a smaller maximum camber improves the robustness in lift to drag ratio, and an airfoil with a larger curvature at the shock wave location improves the robustness in pitching moment against the variation of flight Mach number.

References

[1]Hall, D. W., Parks, R. W., and Morris, S., "Airplane for Mars Exploration," Tech. rep., NASA Ames Research Center, Moffett Federal Airfield, California, May 1997, URL: `http://www.redpeace.org/final_report.pdf`.

[2]Guynn, M. D., Croom, M. A., Smith, S. C., Parks, R. W., and Gelhausen, P. A., "Evolution of a Mars Airplane Concept for the ARES Mars Scout Mission," AIAA Paper 2003–6578, September 2003.

[3]Tanaka, Y., Okabe, Y., Suzuki, H., Nakamura, K., Kubo, D., Tokuhiro, M., and Rinoie, K., "Conceptual Design of Mars Airplane for Geographical Exploration," *Proceedings of the 36th JSASS Annual Meeting*, Tokyo, April 2005, pp. 61–64, in Japanese.

[4]Smith, M. D., Pearl, J. C., Conrath, B. J., and Christensen, P. R., "Thermal Emission Spectrometer Results: Mars Atmospheric Thermal Structure and Aerosol Distribution," *Journal of Geophysical Research*, Vol. 106, No. E10, October 2001, pp. 23929–23945.

[5]Hirota, I., *Global Meteorology*, University of Tokyo Press, Tokyo, 1992, in Japanese.

[6]*iSIGHT Reference Guide Version 7.1*, Engineous Software, Inc., 2002, pp. 220–233.

[7]Deb, K. and Gupta, H., "Searching for Robust Pareto-Optimal Solutions in Multi-objective Optimization," *Evolutionary Multi-Criterion Optimization*, edited by C. A. Coello Coello, A. H. Aguirre, and E. Zitzler, Springer-Verlag, Berlin Heidelberg New York, 2005, pp. 150–164.

[8]Youn, B. D. and Choi, K. K., "Selecting Probabilistic Approaches for Reliability-Based Design Optimization," *AIAA Journal*, Vol. 42, No. 1, January 2004, pp. 124–131.

[9]Koch, P. N., Wujek, B., Golovidov, O., and Simpson, T. W., "Facilitating Probabilistic Multidisciplinary Design Optimization Using Kriging Approximation Models," AIAA Paper 2002–5415, September 2002.

[10]Shimoyama, K., Fujii, K., and Kobayashi, H., "Development of Realistic Optimization Method – Multi-Objective and Robust Optimization," AIAA Paper 2004–4475, August–September 2004.

[11]Deb, K., *Multi-Objective Optimization using Evolutionary Algorithms*, John Wiley & Sons, Ltd., Chichester, 2001.

[12]Shimoyama, K., Oyama, A., and Fujii, K., "A New Efficient and Useful Robust Optimization Approach – Design for Multi-Objective Six Sigma," *Proceedings of the 2005 IEEE Congress on Evolutionary Computation*, Vol. 1, Edinburgh, September 2005, pp. 950–957.

[13]Oyama, A., Obayashi, S., Nakahashi, K., and Hirose, N., "Fractional Factorial Design of Genetic Coding for Aerodynamic Optimization," AIAA Paper 99–3298, June–July 1999.

[14]Fonseca, C. M. and Fleming, P. J., "Genetic Algorithms for Multiobjective Optimization: Formulation, Discussion and Generalization," *Proceedings of the 5th International Conference on Genetic Algorithms*, Morgan Kaufmann Publishers, Inc., San Mateo, California, 1993, pp. 416–423.

[15]Michalewicz, Z., *Genetic Algorithms + Data Structure = Evolution Programs*, Springer-Verlag, Berlin Heidelberg New York, 3rd, Revised and Extended ed., 1996.

[16]Baker, J. E., "Reducing Bias and Inefficiency in the Selection Algorithm," *Proceedings of the 2nd International Conference on Genetic Algorithms*, Morgan Kaufmann Publishers, Inc., San Mateo, California, 1987, pp. 41–49.

[17]Eshelman, L. J. and Schaffer, J. D., "Real-coded Genetic Algorithms and Interval Schemata," *Foundations of Genetic Algorithms 2*, Morgan Kaufmann Publishers, Inc., San Mateo, California, 1993, pp. 187–202.

[18]Eshelman, L. J., "The CHC Adaptive Search Algorithm: How to Have Safe When Engaging in Nontraditional Genetic Recombination," *Foundations of Genetic Algorithms*, Morgan Kaufmann Publishers, Inc., San Mateo, California, 1991, pp. 265–283.

[19]Tsutsui, S. and Fujimoto, Y., "Forking Genetic Algorithms with Blocking and Shrinking modes (fGA)," *Proceedings of the 5th International Conference on Genetic Algorithms*, Morgan Kaufmann Publishers, Inc., San Mateo, California, 1993, pp. 206–213.

[20]Oyama, A., Shimoyama, K., and Fujii, K., "New Constraint-Handling Method for Multi-Objective Multi-Constraint Evolutionary Optimization and Its Application to Space Plane Design," *EUROGEN 2005*, edited by R. Schilling, W. Hasse, J. Periaux, H. Baier, and G. Bugeda, FLM, Munich, September 2005.

[21]Fujii, K. and Obayashi, S., "Practical Applications of New LU-ADI Scheme for the Three-Dimensional Navier-Stokes Computation of Transonic Viscous Flows," AIAA Paper 86–0513, January 1986.

[22]Shima, E. and Jounouchi, T., "Role of CFD in Aeronautical Engineering (No. 14) –AUSM Type Upwind Schemes–," *Proceedings of the 14th NAL Symposium on Aircraft Computational Aerodynamics*, NAL SP–34, Tokyo, January 1997, pp. 7–12.

[23]van Leer, B., "Towards the Ultimate Conservation Difference Scheme. V. A Second-Order Sequel to Godunov's Method," *Journal of Computational Physics*, Vol. 32, 1979, pp. 101–136.

[24]Anderson, W. K., Thomas, J. L., and van Leer, B., "Comparison of Finite Volume Flux Vector Spllittings for the Euler Equations," *AIAA Journal*, Vol. 24, No. 9, September 1986, pp. 1453–1460.

[25]Baldwin, B. S. and Lomax, H., "Thin-Layer Approximation and Algebraic Model for Separated Turbulent Flows," AIAA Paper 78–257, January 1978.